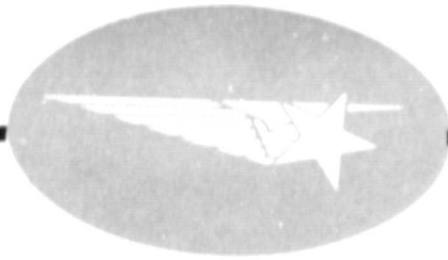


General Disclaimer

One or more of the Following Statements may affect this Document

- This document has been reproduced from the best copy furnished by the organizational source. It is being released in the interest of making available as much information as possible.
- This document may contain data, which exceeds the sheet parameters. It was furnished in this condition by the organizational source and is the best copy available.
- This document may contain tone-on-tone or color graphs, charts and/or pictures, which have been reproduced in black and white.
- This document is paginated as submitted by the original source.
- Portions of this document are not fully legible due to the historical nature of some of the material. However, it is the best reproduction available from the original submission.



N 69-14249

(ACCESSION NUMBER)

(THRU)

49

(PAGES)

1

(CODE)

CR-98137

(NASA CR OR TMX OR AD NUMBER)

21

(CATEGORY)

FACILITY FORM 602

Lockheed

MISSILES & SPACE COMPANY

A GROUP DIVISION OF LOCKHEED AIRCRAFT CORPORATION

SUNNYVALE, CALIFORNIA

HREC/1146-1
LMSC/HREC A791387

LOCKHEED MISSILES & SPACE COMPANY
HUNTSVILLE RESEARCH & ENGINEERING CENTER
HUNTSVILLE RESEARCH PARK
4800 BRADFORD DRIVE, HUNTSVILLE, ALABAMA

INTERIM REPORT
OPTIMUM RENDEZVOUS GUIDANCE STUDY

June 1968

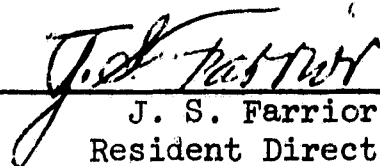
Contract NAS8-21146

by
W. Trautwein
and
J. Waldvogel

APPROVED BY



T. R. Beal, Manager
Dynamics & Guidance



J. S. Farrior
Resident Director

FOREWORD

This report was prepared under Contract NAS8-21146 for the Astrodynamics and Guidance Theory Division, Aero-Astrodynamics Laboratory of the NASA Marshall Space Flight Center.

SUMMARY

This report summarizes LMSC/HREC work in the area of optimum rendezvous guidance. It gives a general review of a simple guidance scheme for minimum fuel rendezvous with two finite burns between a powered intercepting space vehicle in an arbitrary parking orbit and a target vehicle in an essentially coplanar circular orbit.

In Sections 2 through 5 the present form of the guidance concept is outlined as submitted to the AIAA for presentation at the 1968 AIAA Guidance and Control Conference.

Additional details of the studies performed under the contract are given in References 3 through 9.

Major accomplishments during the reporting period were:

- Development and computer check-out of a rapidly converging iteration method that is used for optimum flight scheduling before the first burn and for optimum first burn guidance.
- Extension of the dual phase plane method to long terminal burn times, whereas in its original form application of the method was limited to short burns where the radii of interceptor and target from the earth's center were approximately equal.
- Development, checkout and first utilization of a digital computer program for simulation of complete rendezvous missions with the present guidance scheme used onboard the interceptor.

CONTENTS

Section		Page
	FOREWORD	ii
	SUMMARY	iii
	NOMENCLATURE	1
1	INTRODUCTION	3
2	FIRST BURN GUIDANCE METHOD	5
3	A NUMERICAL METHOD	16
4	TERMINAL GUIDANCE METHOD	19
	4.1 Derivation of Dual Phase Plane Equations of Relative Motion	19
	4.2 Sensitivity of the Optimal Solution to Small Perturbations	32
	4.3 Control Laws for Sensitivity Reduction	34
5	SIMULATION OF RENDEZVOUS MISSIONS	38
	5.1 Flight Scheduling and First Burn Computations	
	5.2 Terminal Guidance	
	5.3 Complete Rendezvous Missions and Comparisons with COV Results	
6	CONCLUSIONS AND RECOMMENDATIONS	
	REFERENCES	

NOMENCLATURE

R		Orbital radius of the target T
ω		Angular velocity of T
α, α_T		Polar angle of the interceptor I, and T respectively
\vec{r}		$(R\cos\alpha_T, R\sin\alpha_T)$ position of T
μ		Gravitational parameter of the earth
\vec{p}_T	=	$(\xi, \eta), \rho = \vec{p} $ position
\vec{s}	=	$(U, V), S = \vec{s} $ velocity
γ		Flight path angle of I
δ		Separation angle between I and T
ϕ		Thrust direction with respect to ξ -axis
χ		Thrust direction with respect to zenith
φ, ψ		Values of χ at beginning and end of the mission, respectively
m		Mass of I
t		Current time
σ, τ		Durations of first and second burn, respectively
Σ	=	$\sigma + \tau$ total burn duration
λ		Mass flow rate
v_x		Exit velocity of the engine of I

τ_x	=	m_0/λ	burn time limit
$\nu(t)$	=	0 or 1	switching function
ω			Mean angular velocity of I during coast
Ω			Polar angle of the pericenter of I's orbit
x, y, z			Coordinates of interceptor relative to target
\vec{r}			Relative slant range vector
\vec{s}			Relative velocity of interceptor
\vec{f}			Thrust per unit mass of interceptor
\vec{f}^*	=	$(2/\omega^2)\vec{f}$	normalized thrust per unit mass
$t^* = \omega t$			Normalized time
$(\cdot), (\cdot)'$			Derivatives with respect to t and t*, respectively
$\bar{e}(t), \bar{h}(t), k(t)$			Criteria for optimal second burn
K_f, K_ϕ			Gain factors for second burn control laws
$\epsilon_f, \epsilon_\phi$			Admissible deviations during second burn

Subscripts

0	Beginning of the rendezvous mission = beginning of the first burn.
1	End of first burn, beginning of coast
2	End of coast, beginning of second burn.
3	End of second burn, rendezvous.
T	Target

Section 1
INTRODUCTION

A wide variety of future space operations including rescue missions to orbiting space vehicles require fast reaction onboard guidance schemes that can steer a powered interceptor I to an unpowered target vehicle T in optimal or near-optimal manner. Such computation schemes should be able to rapidly schedule and start the intercept mission within seconds after receipt of the target ephemeris if the rendezvous is within the propulsion capability of the interceptor. As target acquisition improves during intercept it is desirable that the scheme operates in an adaptive manner where all onboard computations are based on the most recent target and interceptor ephemeris data.

The present paper describes a new guidance scheme for an important particular case of the general rendezvous problem: the adaptive minimum fuel guidance of a variable mass interceptor from any arbitrary elliptical orbit to a target in a coplanar circular orbit.

Most of the proposed onboard rendezvous guidance schemes are based on impulse approximations and classical orbital mechanics. If finite burn durations are considered, optimal rendezvous trajectories may be obtained by applying calculus of variations or modern control theory (Pontryagin). However, the computational load for these methods mostly excludes an implementation onboard.

Rigorous optimal trajectories usually are characterized by a finite number of discrete time intervals of full thrust with coast phases in between. In this paper the simplest case providing a sufficient amount of generality is considered: the burn-coast-burn rendezvous.

For the final guidance it is essential to use relative coordinates between target and interceptor. Only in such a system it is possible to correct errors encountered during the mission, since the control law can be based on measurements of the actual relative position and velocity. Furthermore, the relative coordinates and velocities become small at rendezvous and therefore allow linearization of the equations of motion in the terminal phase. A new technique, the Dual Phase Plane Method (Reference 1), is presented and applied to the second burn control problem. Theoretical insight into the rendezvous as well as very effective and simple guidance laws are obtained in the sequel.

Section 2
THE FIRST BURN

Let the target T of negligible mass move on a circular orbit of radius R about the center \mathcal{O} of the earth, which has the gravitational parameter μ . The constant angular velocity ω of T is related to R by Kepler's third law

$$\omega^2 R^3 = \mu. \quad (2.1)$$

The target T is supposed to be rendezvoused by the interceptor I of initial mass m_0 (negligible compared to the mass of the earth), flying along the trajectory $\vec{p}(t) = \{\xi(t), \eta(t)\}$. The initial configuration is given by the distance ρ_0 of I_0 from \mathcal{O} (See Figure 1), the initial separation angle δ_0 (angle between the radius vectors $\mathcal{O}I_0$ and $\mathcal{O}T_0$), the initial velocity S_0 and the initial flight path angle γ_0 (angle between horizon and velocity vector). Let t_0 and t_3 now be the initial and final time of the whole maneuver, respectively. The engine of I is assumed to burn from the time t_0 to $t_1 = t_0 + \sigma$ ($\sigma > 0$) and from $t_2 = t_3 - \tau$ to t_3 ($\tau > 0$). The total burn time

$$\Sigma = \sigma + \tau \quad (2.2)$$

is supposed to be small with respect to $t_3 - t_0$, if Σ is made as small as possible. Under this assumption it is reasonable to replace the variable thrust direction $\phi(t)$ in each burn period by some average value, which then is kept constant during the burn. More precisely, the assumed constant thrust directions in the first and second burn will be the directions $\phi(t_0)$ and $\phi(t_3)$, respectively, represented by the angles

$$\begin{aligned} \varphi &= \phi(t_0) - \alpha_0 = \chi(t_0) \\ \psi &= \phi(t_3) - \alpha_3 = \chi(t_3) \end{aligned} \quad (2.3)$$

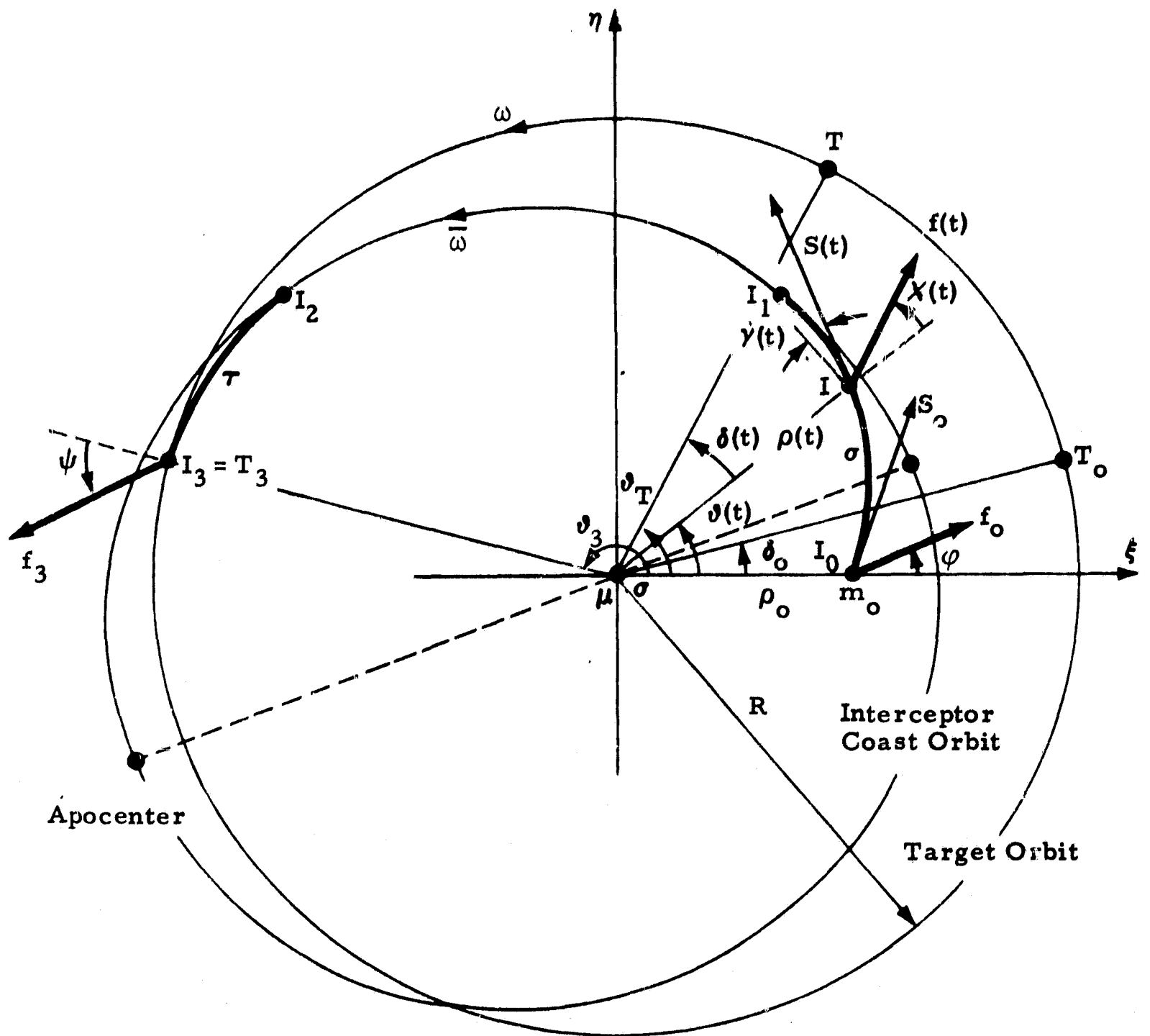


Figure 1 - Notations for the First Burn Guidance Scheme. I_0, I_1, I_2, I_3, I = Positions of the Interceptor at First Ignition, First Cutoff, Second Ignition, Rendezvous or at a General Time, Respectively

where ϑ_0 may be considered as 0, and ϑ_3 is the unknown polar angle of the rendezvous point I_3 .

Thus we are concerned with the problem of determining the control parameters σ , τ , φ , ψ and ϑ_3 such that T and I come to a rendezvous (four conditions) and $\Sigma = \sigma + \tau$ is a minimum. Obviously one degree of freedom is left for minimization.

In order to set up the four rendezvous conditions, we first formulate the equations of motion of I in the Cartesian coordinate system (ξ, η) :

$$\begin{aligned} \dot{\xi} &= U \\ \dot{\eta} &= V \\ \dot{U} &= -\mu \xi / \rho^3 + f(t) \cos \phi \\ \dot{V} &= -\mu \eta / \rho^3 + f(t) \sin \phi \end{aligned} \quad (2.4)$$

where dots denote the differentiation with respect to t, and the thrust acceleration $f(t)$ is given by

$$f(t) = v_x \lambda v(t) / m(t) \quad (2.5)$$

with

$$m(t) = m_0 - \lambda \int_{t_0}^t v(s) ds \quad (2.6)$$

(λ and $v(t)$ are mass flow rate and switching function respectively). By introducing polar coordinates $\rho, \vartheta, \mathcal{S}, \gamma$ according to

$$\begin{aligned} \xi &= \rho \cos \vartheta & \eta &= \rho \sin \vartheta \\ U &= \mathcal{S} \sin(\gamma - \vartheta) & V &= \mathcal{S} \cos(\gamma - \vartheta) \end{aligned}$$

Equations (4) are transformed into

$$\begin{aligned}
 \dot{\rho} &= S \sin \gamma \\
 \dot{\vartheta} &= (S/\rho) \cos \gamma \\
 \dot{S} &= -(\mu/\rho^2) \sin \gamma + f(t) \sin(\gamma + \chi) \\
 \dot{\gamma} &= (S/\rho) \cos \gamma + [(-\mu/\rho^2) \cos \gamma + f(t) \cos(\gamma + \chi)]/S,
 \end{aligned}
 \tag{2.7}$$

where

$$\chi(t) = \phi(t_0) - \vartheta(t) \quad \text{or} \quad \chi(t) = \phi(t_3) - \vartheta(t).$$

Now the data of the interceptor at the end of the first burn, t_1 , are written in terms of the control variables. We use Taylor expansions around $t = t_0$ and truncate them after linear terms since σ is supposed to be small. From (7) it follows immediately:

$$\begin{aligned}
 \rho(t_0 + \sigma) &= \rho_1 = \rho_0 + \sigma S_0 \sin \gamma_0 \\
 \vartheta_1 &= \vartheta_0 + \sigma (S_0/\rho_0) \cos \gamma_0 \\
 S_1 &= S_0 + \sigma [-(\mu/\rho_0^2) \sin \gamma_0 + f_0 \sin(\gamma_0 + \varphi)] \\
 \gamma_1 &= \gamma_0 + (\sigma/S_0) [(\mu E_0/\rho_0^2) \cos \gamma_0 + f_0 \cos(\gamma_0 + \varphi)]
 \end{aligned}
 \tag{2.8}$$

with the abbreviation

$$E_0 = \rho_0 S_0^2 / \mu - 1.
 \tag{2.9}$$

The initial thrust acceleration f_0 can be written as

$$f_0 = v_x / \tau_x \quad (2.10)$$

with the symbol

$$\tau_x = m_0 / \lambda \quad (2.11)$$

according to (5).

Similarly, the state of the interceptor at the beginning of the second burn, t_2 , is represented by truncated Taylor series around $t = t_3$ with time running backwards. Due to the particular situation at $t = t_3$ ($f_3 = 0$, $S_3 = \omega R$) several terms cancel out, and we use the respective expansions up to second order terms:

$$\begin{aligned} \rho(t_3 - \tau) &= \rho_2 = R + \frac{1}{2} \tau^2 f_3 \cos \psi \\ v_2 &= v_3 - \omega \tau + \frac{1}{2} \tau^2 (f_3 / R) \sin \psi \\ S_2 &= \omega R - \tau f_3 \sin \psi + \frac{1}{2} \tau^2 f_3 * \\ &* \left[(f_3 / v_x) \sin \psi - 2 \omega \cos \psi + (f_3 / (\omega R)) \cos^2 \psi \right] \\ \gamma_2 &= (f_3 / (\omega R)) \left\{ -\tau \cos \psi \right. \\ &\left. + \frac{1}{2} \tau^2 \left[(f_3 / v_x) \cos \psi + 3 \omega \sin \psi - (f_3 / (\omega R)) \sin 2 \psi \right] \right\} \end{aligned} \quad (2.12)$$

where

$$f_3 = v_x / (\tau_x - \Sigma) \quad (2.13)$$

is the final thrust acceleration.

Now the conditions for rendezvous are established by equating the orbital elements given by position and velocity of the interceptor at the times t_1 and t_2 respectively (based on the approximations (8) and (12)). First, by considering the inverse semi-major axis (energy)

$$\frac{1}{a} = \frac{2}{\rho} - \frac{S^2}{\mu} \quad (2.14)$$

of the coasting ellipse, we obtain

$$\frac{2}{\rho_0} - \frac{S_0^2}{\mu} - 2\sigma \frac{S_0 f_0}{\mu} \sin(\gamma_0 + \varphi) = \frac{1}{R} + 2\tau \frac{\omega R f_0}{\mu} \sin \psi, \quad (2.15)$$

when again only first order terms in σ, τ are taken into account.

Then, the "second Laplace vector" (Reference 2) in complex notation is used for obtaining the eccentricity \mathcal{E} of the coasting ellipse and the true anomalies Ω_1, Ω_2 of the points I_1, I_2 . Generally, the complex number

$$\zeta = e^{i\gamma} (E \cos \gamma + i \sin \gamma) \quad (2.16)$$

(with E from (9)) indicates by its magnitude the eccentricity \mathcal{E} of the ellipse given by ρ, S, γ , and by its argument the true anomaly Ω of that point:

$$\zeta = \epsilon \cdot e^{i\Omega} \quad (2.17)$$

Thus, by inserting (8) and (12) into (16), we obtain for the truncated series of ζ, \mathcal{E} and Ω at the points I_1, I_2 :

$$\begin{aligned} \zeta_1 &= e^{i\gamma_0} (E_0 \cos \gamma_0 + i \sin \gamma_0) \\ &\quad + \frac{\sigma S_0}{\rho_0} \left[i e^{i\gamma_0} \cos \gamma_0 (E_0 \cos \gamma_0 + i \sin \gamma_0) \right. \\ &\quad \left. + \frac{\rho_0^2 f_0}{\mu} (\sin \varphi e^{i\gamma_0} + i \cos \gamma_0 e^{-i\varphi}) \right] \\ \mathcal{E}_1 &= \mathcal{E}_0 + \frac{\sigma \rho_0 S_0 f_0}{\mu \mathcal{E}_0} \cos \gamma_0 \left[\mathcal{E}_0 (\sin \varphi + \sin(\gamma_0 + \varphi) \cos \gamma_0) \right. \\ &\quad \left. + \cos(\gamma_0 + \varphi) \sin \gamma_0 \right]; \quad \mathcal{E}_0 \neq 0 \\ \Omega_1 &= \Omega_0 + \sigma S_0 \left\{ \frac{\cos \gamma_0}{\rho_0} \right. \\ &\quad \left. + \frac{\rho_0 f_0}{\mu \mathcal{E}_0^2} \left[(\mathcal{E}_0 + 1) \cos^2 \gamma_0 \cos(\gamma_0 + \varphi) - \cos(\gamma_0 - \varphi) \right] \right\} \end{aligned} \quad (2.18)$$

with

$$\varepsilon_0 = \sqrt{E_0^2 \cos^2 \gamma_0 + \sin^2 \gamma_0} \quad (2.19)$$

$$\Omega_0 = \gamma_0 + \arg(E_0 \cos \gamma_0 + i \sin \gamma_0)$$

and

$$\zeta_2 = \frac{\tau f_3}{\omega R} \left\{ -2 \sin \psi - i \cos \psi + \frac{\tau}{2} \left[\frac{f_3}{v_x} (2 \sin \psi + i \cos \psi) + i \frac{2 f_3}{\omega R} \sin \psi e^{-i\psi} - 3 \omega e^{i\psi} \right] \right\} \quad (2.20)$$

$$\varepsilon_2 = \frac{\tau f_3}{\omega R} \sqrt{1 + 3 \sin^2 \psi}$$

$$\Omega_2 = \arg(-2 \sin \psi - i \cos \psi) - \tau \frac{\frac{3}{2} \omega (1 + \sin^2 \psi) + \frac{f_3}{\omega R} \sin^2 \psi \cos \psi}{1 + 3 \sin^2 \psi}.$$

The formulas for ε_1 , Ω_1 , Ω_0 in (18), (19) are not applicable when the first burn is started on a circular or near-circular orbit around the earth:

$$\gamma_0 = 0, \quad E_0 = 0.$$

A second order analysis (Reference 3) shows that for sufficiently small values of ε_0 the correct limits (18) and (19) are obtained by putting

$$\varepsilon_0 = \frac{2\kappa \sin \varphi}{\sqrt{1 + 3 \sin^2 \varphi}}, \quad \tan \gamma_0 = \frac{\kappa \cos \varphi}{\sqrt{1 + 3 \sin^2 \varphi}} \quad (2.21)$$

where κ is a sufficiently small quantity.

A second rendezvous condition is now obtained by equating the eccentricities ($\epsilon_1 = \epsilon_2$):

$$\begin{aligned} \epsilon_0 + \frac{\sigma \rho_0 S_0 f_0}{\mu \epsilon_0} \cos \gamma_0 [E_0 (\sin \varphi + \sin(\gamma_0 + \varphi) \cos \gamma_0) + \cos(\gamma_0 + \varphi) \sin \gamma_0] \\ = \frac{\tau f_3}{\omega R} \sqrt{1 + 3 \sin^2 \psi} \end{aligned} \quad (2.22)$$

with ϵ_0 from (19), and by requiring agreement in the polar angle of the pericenter, $\vartheta_1 - \Omega_1 = \vartheta_2 - \Omega_2$, we obtain as a third condition the equation

$$\vartheta_3 - \vartheta_0 = \sigma \frac{S_0}{\rho_0} \cos \gamma_0 + \omega \tau + \Omega_2 - \Omega_1, \quad (2.23)$$

with Ω_1, Ω_2 from (18), (20), which may be used for computing the location of the rendezvous point.

The fourth condition, which forces T and I to reach their final positions simultaneously, is established by using a first order approximation of Kepler's equation,

$$\bar{\omega} (t_2 - t_1) = \Omega_2 - \Omega_1 - 2\epsilon (\sin \Omega_2 - \sin \Omega_1) + \dots,$$

where

$$\bar{\omega} = \sqrt{\frac{\mu}{a^3}}$$

[a from (14)] is the mean angular velocity of the interceptor on the coasting ellipse. After straight-forward computations using first order terms only we obtain

$$\begin{aligned} \sigma \left(\frac{S_0}{\rho_0} \cos \gamma_0 - \omega \right) + \frac{3\tau f_3}{\omega R} (\Omega_2 - \Omega_1) \sin \psi \\ - \frac{2\tau f_3}{\omega R} \cos \psi - \frac{\tau f_3}{\omega R} \sqrt{1 + 3 \sin^2 \psi} \cdot \frac{\rho_0 S_0^2}{\mu \epsilon_0} \sin 2\gamma_0 \\ = \sigma_0. \end{aligned} \quad (2.24)$$

To sum up, (15), (22), (24) form a system of three equations

$$\begin{aligned} a_0 + f_0 a_1 \sigma + f_3 a_2 \tau &= 0 \\ b_0 + f_0 b_1 \sigma + f_3 b_2 \tau &= 0 \\ c_0 + f_0 c_1 \sigma + f_3 c_2 \tau &= 0 \end{aligned} \quad (2.25)$$

for $\sigma, \tau, \varphi, \psi$, where

$$f_0 = \frac{v_x}{\tau_x}, \quad f_3 = \frac{v_x}{\tau_x - \sigma - \tau}$$

and

$$\begin{aligned} a_0 &= \frac{1}{R} - \frac{2}{\rho_0} + \frac{S_0^2}{\mu} \\ a_1(\varphi) &= \frac{2}{\mu} S_0 + \sin(\gamma_0 + \varphi) \\ a_2(\psi) &= \frac{2}{\mu} \omega R \sin \psi \\ b_0 &= \sqrt{E_0^2 \cos^2 \gamma_0 + \sin^2 \gamma_0} \\ b_1(\varphi) &= \frac{\rho_0 \cos \gamma_0}{S_0 b_0} (E_0 + 1) \left[E_0 (\sin \varphi + \sin(\gamma_0 + \varphi) \cos \gamma_0) \right. \\ &\quad \left. + \cos(\gamma_0 + \varphi) \sin \gamma_0 \right] \\ b_2(\psi) &= -\frac{1}{\omega R} \sqrt{1 + 3 \sin^2 \psi} \\ c_0 &= d_0 \\ c_1 &= \frac{1}{f_0} \left(\omega - \frac{S_0}{\rho_0} \cos \gamma_0 \right) \\ c_2(\psi) &= \frac{1}{\omega R} \left[2 \cos \psi - 3(\Omega_2 - \Omega_1) \sin \psi \right. \\ &\quad \left. + \frac{E_0 + 1}{b_0} \cdot \sin 2\gamma_0 \sqrt{1 + 3 \sin^2 \psi} \right] \end{aligned} \quad (2.26)$$

with

$$\begin{aligned} \Omega_1 &= \gamma_0 + \arg(E_0 \cos \gamma_0 + i \sin \gamma_0), \quad -\frac{\pi}{2} \leq \Omega_1 < \frac{3\pi}{2} \\ \Omega_2(\psi) &= \arg(-2 \sin \psi - i \cos \psi), \quad \frac{\pi}{2} \leq \Omega_2 < \frac{5\pi}{2} \quad (2.27) \\ E_0 &= \rho_0 S_0^2 / \mu - 1. \end{aligned}$$

When b_0 from (26) turns out to be smaller than .1, use the substitute values for E_0 ; γ_0 according to (21). The restrictions on Ω_1 , Ω_2 exclude the cases where the whole mission would take longer than one revolution of the target. The system (25) has to be satisfied while the total burn time $\Sigma = \sigma + \tau$ is minimized.

The condition that (25) can be satisfied by quantities $(f_0 \sigma)$, $(f_3 \tau)$ is

$$\begin{vmatrix} a_0 & a_1 & a_2 \\ b_0 & b_1 & b_2 \\ c_0 & c_1 & c_2 \end{vmatrix} = 0. \quad (2.28)$$

By expanding this determinant with respect to the third line (28) may be written as

$$G(\varphi, \psi) = c_0 D_0 + c_1 D_1 + c_2 D_2 = 0 \quad (2.29)$$

where

$$\begin{aligned} D_0 &= a_1 b_2 - a_2 b_1 \\ D_1 &= a_2 b_0 - a_0 b_2 \\ D_2 &= a_0 b_1 - a_1 b_0. \end{aligned} \quad (2.30)$$

Provided (29) is satisfied, the system (25) can be solved for σ , τ by taking only two of the three equations, for instance the first and the second one. By Cramer's rule we immediately obtain the relations

$$f_0 \sigma = \frac{D_1}{D_0}, \quad f_3 \tau = \frac{v_x \tau}{\tau_x - \sigma - \tau} = \frac{D_2}{D_0},$$

from which there follows

$$\sigma = \frac{1}{f_0} \frac{D_1}{D_0}, \quad \tau = \frac{1}{f_0} \frac{D_2}{D_0} \frac{D_0 - \frac{D_1}{v_x}}{D_0 + \frac{D_2}{v_x}} \quad (2.31)$$

and

$$\sum(\varphi, \psi) = \sigma + \tau = \frac{D_1 + D_2}{D_0 + \frac{D_2}{v_x}}. \quad (2.32)$$

Thus, the on-board computing scheme consists of minimizing $\sum(\varphi, \psi)$ (given by (32)) by varying φ , ψ , while the equation $G(\varphi, \psi) = 0$ (see (29)) must hold.

These computations may be carried out even before starting the first burn. Then, all important data about the planned mission, such as approximate duration, fuel consumption, location of the rendezvous point are obtained. If no minimum of \sum with $G = 0$ and $\sigma \geq 0$, $\tau \geq 0$ can be found, the mission would extend over more than one revolution of the target, or this simplified theory is not applicable.

During the first burn the minimization is repetitively carried out using updated position and velocity data of the interceptor. As the remaining burn duration decreases, the accuracy of the above approximations increases.

Section 3
A NUMERICAL METHOD

The objective of this section is to develop a numerical method which allows us to solve the minimum problem

$$\Sigma(x,y) = \min, \quad G(x,y) = 0 \quad (3.1)$$

without computation of the partial derivatives of Σ and G . In order to obtain the solution of (1) analytically, we would preferably choose the method of the Lagrange multipliers since generally the side-condition $G(x,y) = 0$ cannot be solved for x or y in a closed form. This method requires to minimize the function

$$\Psi(x,y,\Lambda) = \Sigma(x,y) - \Lambda G(x,y) \quad (3.2)$$

by variation of x , y and the Lagrange multiplier Λ . Thus, the conditions

$$\Sigma_x - \Lambda G_x = 0, \quad \Sigma_y - \Lambda G_y = 0, \quad G = 0 \quad (3.3)$$

for the unknowns x , y , Λ are obtained (the subscripts x , y denote differentiation with respect to x or y respectively). By eliminating Λ between the first two of these equations, (3) is reduced to the two variable system

$$\begin{aligned} \Sigma_x(x,y) \cdot G_y(x,y) - \Sigma_y(x,y) \cdot G_x(x,y) &= 0 \\ G(x,y) &= 0. \end{aligned} \quad (3.4)$$

This system may be solved iteratively by improving an initial guess x_0, y_0 of the solution using linearization of (4) at the point (x_0, y_0) (method of Newton-Raphson). By putting

$$x = x_0 + \Delta x, \quad y = y_0 + \Delta y \quad (3.5)$$

the linearized form of (4) becomes

$$\begin{aligned} \sum_x G_y - \sum_y G_x + \Delta x (\sum_x G_y - \sum_y G_x)_x + \Delta y (\sum_x G_y - \sum_y G_x)_y &= 0 \\ G + \Delta x \cdot G_x + \Delta y \cdot G_y &= 0 \end{aligned}$$

or

$$\begin{aligned} \sum_x G_y - \sum_y G_x + \Delta x (\sum_{xx} G_y - G_{xx} \sum_y - \sum_{xy} G_x + G_{xy} \sum_x) \\ + \Delta y (-\sum_{yy} G_x + G_{yy} \sum_x + \sum_{xy} G_y - G_{xy} \sum_y) &= 0 \quad (3.6) \\ G + \Delta x \cdot G_x + \Delta y \cdot G_y &= 0, \end{aligned}$$

where all functions and derivatives must be taken at the point (x_0, y_0) . From this system of two linear equations the increments Δx , Δy can be determined, provided that its determinant does not vanish. It is well known that the iteration of these operations yields a quadratically convergent process.

We now assume that the partial derivatives occurring in (6) are computed approximately by numerical differentiation using 2 or 3 values of the functions \sum , G . A detailed analysis shows that the truncation errors introduced by this numerical differentiation do not spoil the superlinear convergence of the Newton-Raphson method. It can be shown (Reference 8) that the iteration we are going to propose has a convergence exponent of at least $\sqrt{2}$. However, the round off errors due to numerical differentiation may reduce the accuracy of the final result (this usually happens when minimum problems are solved without analytical differentiation).

In order to establish the derivatives we need in (6) we assume that the values of the functions $\sum(x,y)$, $G(x,y)$ are known at the 9 points.

$$\begin{aligned} (x_i, y_j), \quad i, j = 0, 1, 2 \\ x_1 = x_0 + h, \quad x_2 = x_0 - h, \quad y_1 = y_0 + k, \quad y_2 = y_0 - k \end{aligned} \quad (3.7)$$

and are denoted by

$$\Sigma_{ij} = \Sigma(x_i, y_j), \quad G_{ij} = G(x_i, y_j), \quad i, j = 0, 1, 2$$

(h and k are the step lengths in the x and y direction respectively). From these values we get the following approximations for the respective partial derivatives at the point (x_0, y_0)

$$\begin{aligned} \Sigma_x &\cong \frac{1}{2h} (\Sigma_{10} - \Sigma_{20}) \\ \Sigma_y &\cong \frac{1}{2k} (\Sigma_{01} - \Sigma_{02}) \\ \Sigma_{xx} &\cong \frac{1}{h^2} (\Sigma_{10} - 2\Sigma_{00} + \Sigma_{20}) \\ \Sigma_{xy} &\cong \frac{1}{4hk} (\Sigma_{11} - \Sigma_{21} - \Sigma_{12} + \Sigma_{22}) \\ \Sigma_{yy} &\cong \frac{1}{k^2} (\Sigma_{01} - 2\Sigma_{00} + \Sigma_{02}) \end{aligned} \tag{3.8}$$

and similar expressions for the function G. These may readily be substituted into (6) thus making a system of two linear equations for Δx , Δy involving only the 18 function values Σ_{ij} , G_{ij} ($i, j = 0, 1, 2$). By (5) a new approximative solution (x, y) of the system (4) is obtained. If the initial guess (x_0, y_0) and the step lengths h, k are properly chosen, the new approximation is better than the old one.

An iterative procedure is generated by selecting among the 9 points (x_i, y_j) the point (x_{i_0}, y_{j_0}) which is nearest to (x, y) and by assigning the values x_{i_0} , y_{j_0} to the variables x_1 , y_1 respectively. If the values of x , y are assigned to the variables x_0 , y_0 , the whole frame (x_i, y_j) , $i, j = 0, 1, 2$ can be redefined according to (7). This terminates one cycle of the iteration.

Application of this technique to cases of the particular minimum problem of Section 2 gave values of φ , ψ with an accuracy of 4 decimals within a few iteration steps. Convergence was achieved even if the solution turned out to lie considerably outside the rectangle of the initial guesses defined in (7).

Section 4

TERMINAL GUIDANCE METHOD

The terminal rendezvous guidance problem is usually treated using a rotating frame of relative coordinates centered at the target with one axis in the direction of the target zenith (Reference 5).

An attractive phase plane representation that provides good insight into the terminal approach dynamics can be gained if the equations of relative motion are derived in a target centered frame of relative coordinates with space fixed orientation. Simple guidance logic for terminal burn switching and steering results from this new formulation.

The basic dual phase plane concept (Reference 1) based upon the simplifying assumption of equal distance of target and interceptor from the dynamic center is presented here in an extended form where first-order gravitational effects are included as in the usual Clohessy-Wiltshire formulation.

4.1 DERIVATION OF DUAL PHASE PLANE EQUATIONS OF RELATIVE MOTION

It is assumed that thrust per unit mass and the steering angle ϕ are approximately constant during terminal burn and that the interceptor has some a priori information of the predicted location of the rendezvous point. The first burn guidance scheme can provide such an estimate in the present approach.

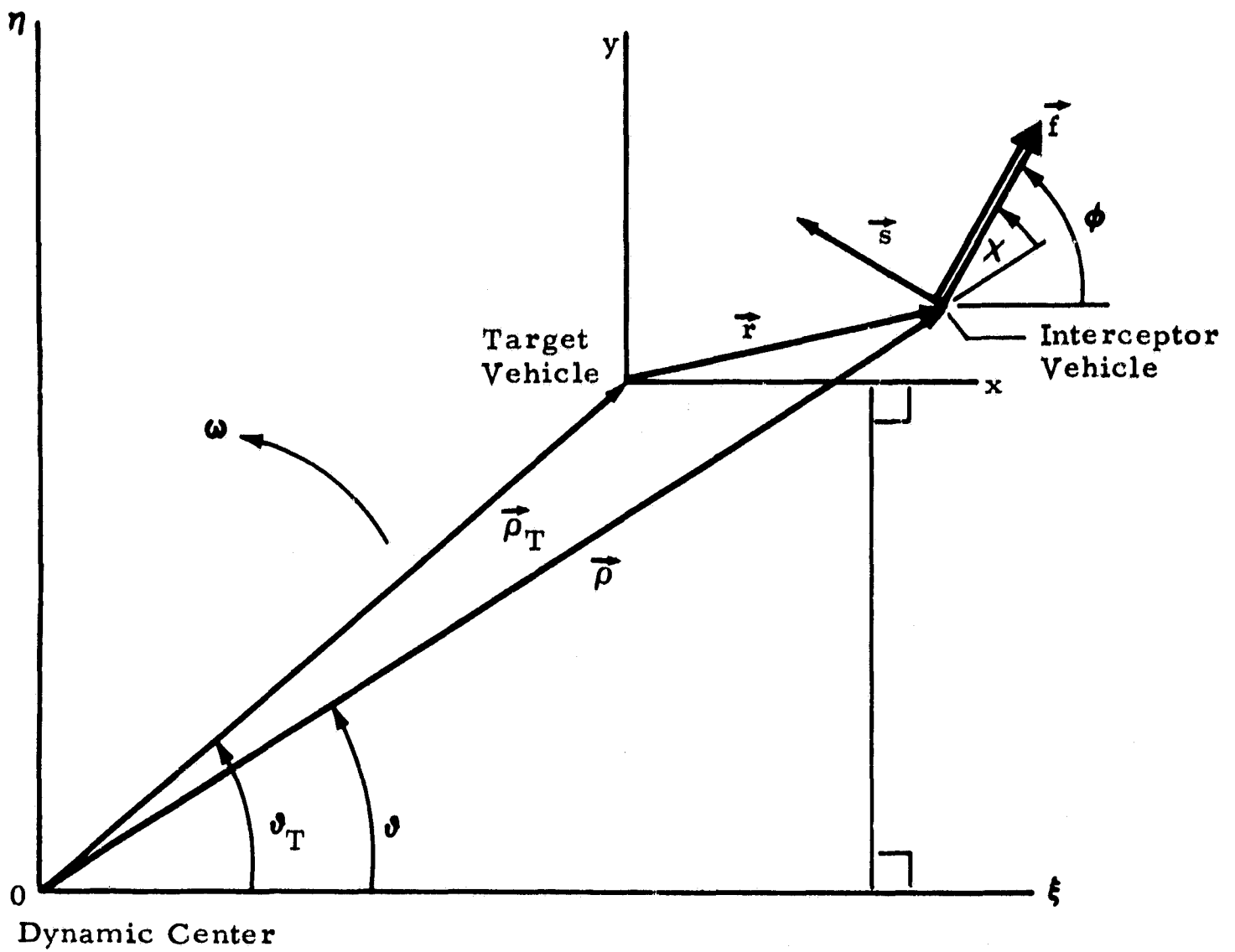


Figure 2 - Target-Referenced Relative Coordinates (x, y, z) with Inertially Fixed Orientation (x, y-projection)

for the target and

$$\ddot{\vec{\rho}} = -\mu \frac{\vec{\rho}}{\rho^3} + \vec{f} \quad (4.2)$$

for the interceptor.

The motion of the interceptor relative to the target is obtained by subtracting the accelerations of Equations (4.1) and (4.2):

$$\begin{aligned} \ddot{\vec{r}} &= \ddot{\vec{\rho}} - \ddot{\vec{\rho}}_T \\ \ddot{\vec{r}} &= -\mu \left(\frac{\vec{\rho}}{\rho^3} - \frac{\vec{\rho}_T}{R^3} \right) + \vec{f} \end{aligned} \quad (4.3)$$

Resolving the vectors into their components yields:

$$\vec{r} = \begin{pmatrix} x \\ y \end{pmatrix}; \quad \vec{\rho} = \begin{pmatrix} \xi \\ \eta \end{pmatrix} = \begin{pmatrix} R \cos \vartheta_T + x \\ R \sin \vartheta_T + y \end{pmatrix}, \quad (4.4)$$

$$\vec{\rho}_T = \begin{pmatrix} \xi \\ \eta \end{pmatrix} = \begin{pmatrix} R \cos \vartheta_T \\ R \sin \vartheta_T \end{pmatrix}; \quad \vec{f} = \begin{pmatrix} f \cos \phi \\ f \sin \phi \end{pmatrix}.$$

Substituting Equation (4.4) into Equation (4.3) yields the scalar form of the dynamic Equation (4.3)

$$\ddot{x} = -\mu \left(\frac{\xi}{\rho^3} - \frac{\xi_T}{R^3} \right) + f \cos \phi, \quad (4.5)$$

$$\ddot{y} = -\mu \left(\frac{\eta}{\rho^3} - \frac{\eta_T}{R^3} \right) + f \sin \phi \quad (4.6)$$

Since,

$$\rho^2 = R^2 \left[1 + \frac{2}{R} (x \cos \vartheta_T + y \sin \vartheta_T) + \left(\frac{r}{R} \right)^2 \right],$$

a first-order approximation that is valid when $r \ll R$ can be obtained:

$$\frac{1}{\rho^3} \approx \frac{1}{R^3} \left[1 - \frac{3}{R} (x \cos \vartheta_T + y \sin \vartheta_T) \right]. \quad (4.7)$$

Assuming a circular target orbit, where

$$\frac{\mu}{R^3} = \omega^2, \quad (4.8)$$

eliminating ξ and η , and substituting Equations (4.7) and (4.8) into Equation (4.5) yields

$$\ddot{x} = -\omega^2 \left\{ (R \cos \vartheta_T + x) \left[1 - \frac{3}{R} (x \cos \vartheta_T + y \sin \vartheta_T) \right] - R \cos \vartheta_T \right\} + f \cos \phi,$$

$$\ddot{y} = -\omega^2 \left\{ (R \sin \vartheta_T + y) \left[1 - \frac{3}{R} (x \cos \vartheta_T + y \sin \vartheta_T) \right] - R \sin \vartheta_T \right\} + f \sin \phi.$$

Again neglecting second-order terms yields

$$\ddot{x} = -\omega^2 \left[x - 3 \cos \vartheta_T (x \cos \vartheta_T + y \sin \vartheta_T) \right] + f \cos \phi , \quad (4.9)$$

$$\ddot{y} = -\omega^2 \left[y - 3 \sin \vartheta_T (x \cos \vartheta_T + y \sin \vartheta_T) \right] + f \sin \phi . \quad (4.10)$$

These equations of relative motion can be substantially simplified if the inertial reference direction of the (ξ, η) - and (x, y) -frames is chosen such that

$$\vartheta_T - k \frac{\pi}{2} \ll 1 \quad \text{for } t \rightarrow t_3 , \quad (4.11)$$

where $k = 0, 1, 2$ or 3 .

Specifying the inertial reference for the terminal flight phase ($t \rightarrow t_3$) in this way does not complicate the onboard computing work because this reference is used after the first burn guidance scheme has predicted the approximate position of the rendezvous point. Therefore the x -axis may be aligned after the first burn along the predicted zenith of the rendezvous point [$k = 0$ in Equation (4.11)].

Assuming $\vartheta_T \ll 1$ for $t_2 < t < t_3$, the small angle approximation $\sin \vartheta_T \approx \vartheta_T$, $\cos \vartheta_T \approx 1$, can be used and all second-order terms such as $x\vartheta_T$, $y\vartheta_T$ are dropped again. Thus the following equations of relative motion result:

$$\ddot{x} = 2\omega^2 x + f \cos \phi \quad (4.12a)$$

$$\ddot{y} = -\omega^2 y + f \sin \phi \quad (4.12b)$$

Equations (4.12) describe the interceptor motion relative to the target in the nonrotating (x, y, z) -frame based on the simplifying assumptions

$$r \ll R, \quad \vartheta_T \ll 1,$$

and corresponding first-order expansions throughout the derivation.

A comparison of Equations (4.12) with the usual Clohessy-Wiltshire equations of relative motion (Reference 5) based on a rotating frame (x -axis aligned with target zenith):

$$\ddot{x} = 3\omega^2 x - 2\omega\dot{y} + f \cos \phi$$

$$\ddot{y} = 2\omega\dot{x} + f \sin \phi$$

reveals the basic advantage of the nonrotating frame used here where no coupling terms due to Coriolis forces are present and the steering angle is the only coupling variable for x - and y -motion. Therefore, Equations (4.12a) and (4.12b) lend themselves to straightforward phase plane representation similar to the basic approach of Reference 1.

To this end, Equations (4.12a) and (4.12b) are rewritten in terms of x, u and y, v , respectively, for representation in an x, u and y, v phase plane (primes denote derivatives with respect to $t^* = \omega t$, $u \triangleq dx/dt^*$, $v \triangleq dy/dt^*$):

$$\left. \begin{aligned} x'' &= u' = u \frac{du}{dx} = 2x + \frac{f \cos \phi}{\omega^2} \\ y'' &= v' = v \frac{dv}{dy} = -y + \frac{f \sin \phi}{\omega^2} \end{aligned} \right\} \quad (4.13)$$

Integrating under the simplifying assumption of constant thrust per unit mass and constant ϕ leads to the following trajectories through the phase plane origin:

$$u^2 = 2x^2 + 2 \frac{f}{\omega^2} x \cos \phi \quad (4.14)$$

$$v^2 = -y^2 + 2 \frac{f}{\omega^2} y \sin \phi \quad (4.15)$$

Hence, the x, u -motion of Equation (4.14) follows a hyperbolic path. The y, v -motion follows a circular arc in the zero miss distance case. This is better shown in the standard forms and displayed in Figure 3:

$$\frac{\left(x + \frac{f}{2\omega^2} \cos \phi\right)^2}{\left(\frac{f}{2\omega^2} \cos \phi\right)^2} - \frac{u^2}{\left(\frac{f}{\sqrt{2}\omega^2} \cos \phi\right)^2} = 1, \quad (4.16)$$

$$\left(y - \frac{f}{\omega^2} \sin \phi\right)^2 + v^2 = \frac{f^2}{\omega^4} \sin^2 \phi. \quad (4.17)$$

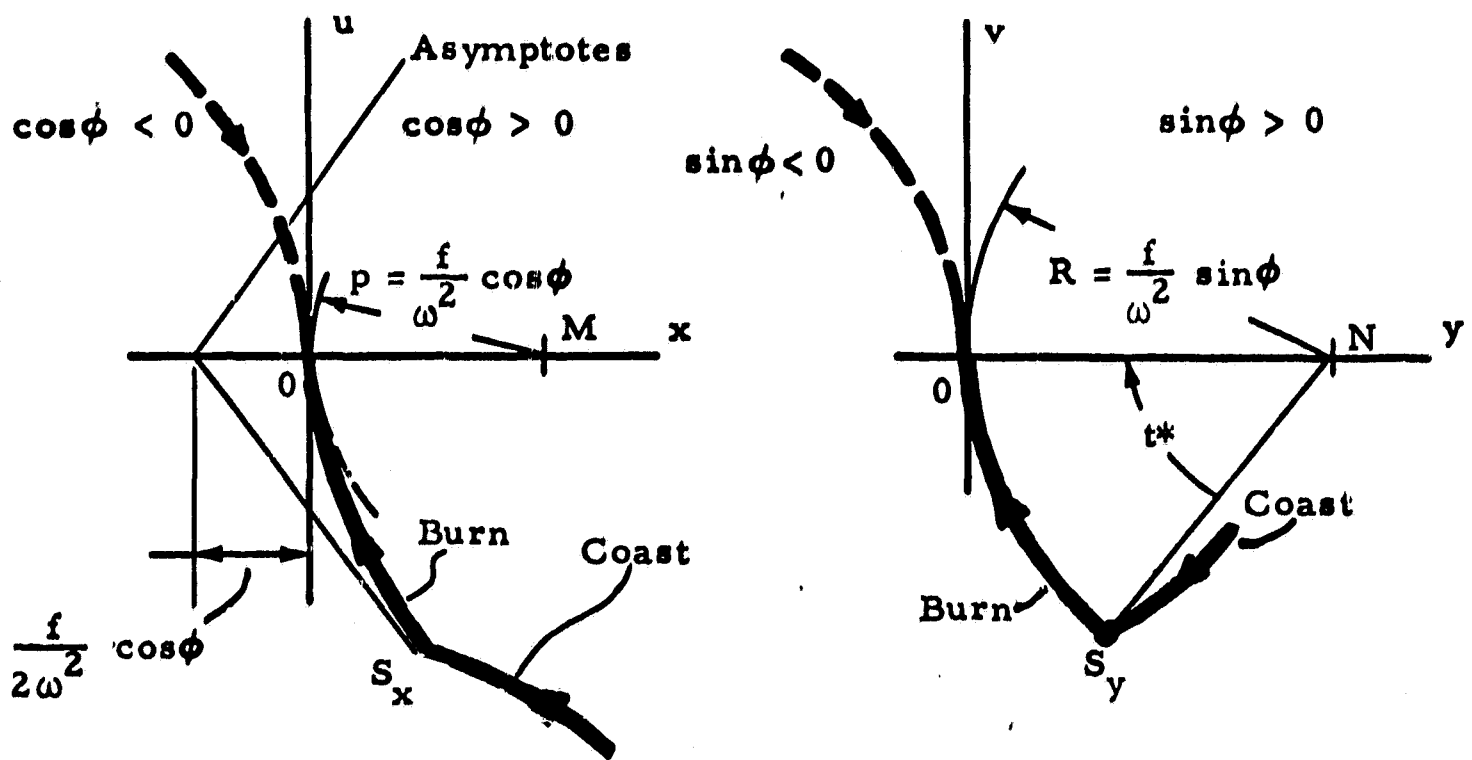


Figure 3 - Phase Trajectories of Optimal Hyperbolic x-Motion and Optimal Circular y-Motion During Terminal Powered Flight Phase

Characteristics of the x, u-Phase Trajectory

The optimal hyperbolic x, u-trajectories, Equation (4.16), have the asymptotes (note $u = dx/t^*$; $t^* = \omega t$):

$$u = \pm \sqrt{2} \left(x + \frac{f}{2\omega^2} \cos\phi \right) ,$$

and the semilatus rectum

$$p = \frac{b^2}{a} = \frac{f}{\omega^2} \cos\phi ,$$

which is also the radius R_x of the trajectories in the origin.

The time from a given point S on the hyperbola with ordinate u_s for a phase point to reach the origin is

$$t_s^* = -\frac{\sqrt{2}}{2} \operatorname{arc\,sinh} \frac{\sqrt{2} \omega^2}{f \cos\phi} u_s . \quad (4.18)$$

Characteristics of the y, v-Phase Trajectory

The optimal y, v-trajectories, Equation (4.17), are circles through the origin with radius

$$R_y = \frac{f}{\omega^2} \sin\phi .$$

The time t^* for a phase point to reach the origin along the optimal path from a given point S with coordinates y_s, v_s is represented by the polar angle of its radius vector from the center of the circle as shown in Figure 3 or

$$t^* = -\operatorname{arc\,sin} \frac{\omega^2}{f \sin\phi} v_s .$$

Conditions for Optimal Second Burn Trajectories

In terms of the above phase plane representation the necessary and sufficient conditions for minimum fuel, i.e., time optimal powered terminal flight phase under the simplifying assumptions ($f \approx \text{const}$, $\phi \approx \text{const}$) made can be stated as follows:

Condition I:

During second burn the x, u-phase point must follow a hyperbolic path, the y, v-phase point must follow a circular path both of which pass through the origin.

An analytical representation of Condition I is gained from combining Equations (4.16) and (4.17), which results in the following vector equation:

$$\vec{r}^* - \vec{f}^* = 0 \quad (4.19)$$

where for convenience the following new vectors are used

$$\begin{aligned} \vec{f}^* &= \begin{pmatrix} f_x^* \\ f_y^* \end{pmatrix} = \begin{pmatrix} \frac{2f}{\omega^2} \cos\phi \\ \frac{2f}{\omega^2} \sin\phi \end{pmatrix} \\ \vec{r}^* &= \begin{pmatrix} x^* \\ y^* \end{pmatrix} = \begin{pmatrix} x(-2 + \frac{u^2}{x^2}) \\ y(1 + \frac{v^2}{y^2}) \end{pmatrix} \\ \vec{g}^* &= \begin{pmatrix} u^* \\ v^* \end{pmatrix} = \begin{pmatrix} u(-2 + \frac{u^2}{x^2}) \\ v(1 + \frac{v^2}{y^2}) \end{pmatrix} \end{aligned} \quad (4.20)$$

Equation (4.19) is broken down into an angular relation

$$g \triangleq \vec{r}^* \times \vec{f}^* = 0 \quad (4.21)$$

and a scalar equation

$$h \triangleq r^{*2} - f^{*2} = 0 \quad (4.22)$$

Equation (4.22) is independent of the steering angle ϕ and ideally suited as a switching function for second burn switching:

$$\nu = \begin{cases} 0 & \text{for } h < 0 \\ 1 & \text{for } h \geq 0 \end{cases} \quad (4.23)$$

Condition II:

The two phase points must reach the origin simultaneously. Hence, for any time t^* during second burn the relation

$$k \triangleq \arcsin 2 \frac{v(t^*)}{f_y^*} - \frac{\sqrt{2}}{2} \operatorname{arcsinh} 2\sqrt{2} \frac{u(t^*)}{f_x^*} = 0 \quad (4.24)$$

must hold.

For sufficiently short second burn times where the hyperbolic x, u -path can be approximated by the circle with radius p condition II reduces to the simple form:

$$u f_y^* - v f_x^* \approx 0$$

or

$$\vec{s} \times \vec{f}^* \approx 0$$

or, in view of Equation (4.21)

$$\tilde{k} \triangleq \vec{s} \times \vec{r}^* \approx 0 \quad (4.24a)$$

Equation (4.24a) is an approximation of condition (4.24) for small burn times. From simple geometrical considerations (Figure 4), an additional relation can be derived for the approach phase (Reference 1): x, y and y, v motion in the superimposed x, u - and y, v -phase planes (or "dual phase plane") must be aligned with the origin. Hence,

$$x v - y u \approx 0$$

or

$$\vec{r} \times \vec{s} \approx 0$$

Optimal terminal guidance can thus be accomplished in the following way:

- During coast compute the switching function h , Equation (4.22), using the target-oriented frame of Figure 2 for defining the relative coordinates. The x -axis must be approximately aligned with the zenith of the predicted rendezvous point.
- Start second burn if switching criterion (4.23), $h \geq 0$ is satisfied.
- The optimal steering angle is given by Equation (4.21) or

$$\phi^0 = \arctan \frac{y^*}{x^*} \quad (4.25)$$

- For simultaneous zeroing of all relative coordinates condition $k = 0$, Equation (4.24) must hold during second burn. For short burn times, Equation (4.24) can be approximated by Equation (4.24a)

$$\tilde{k} = 0 \quad (4.26)$$

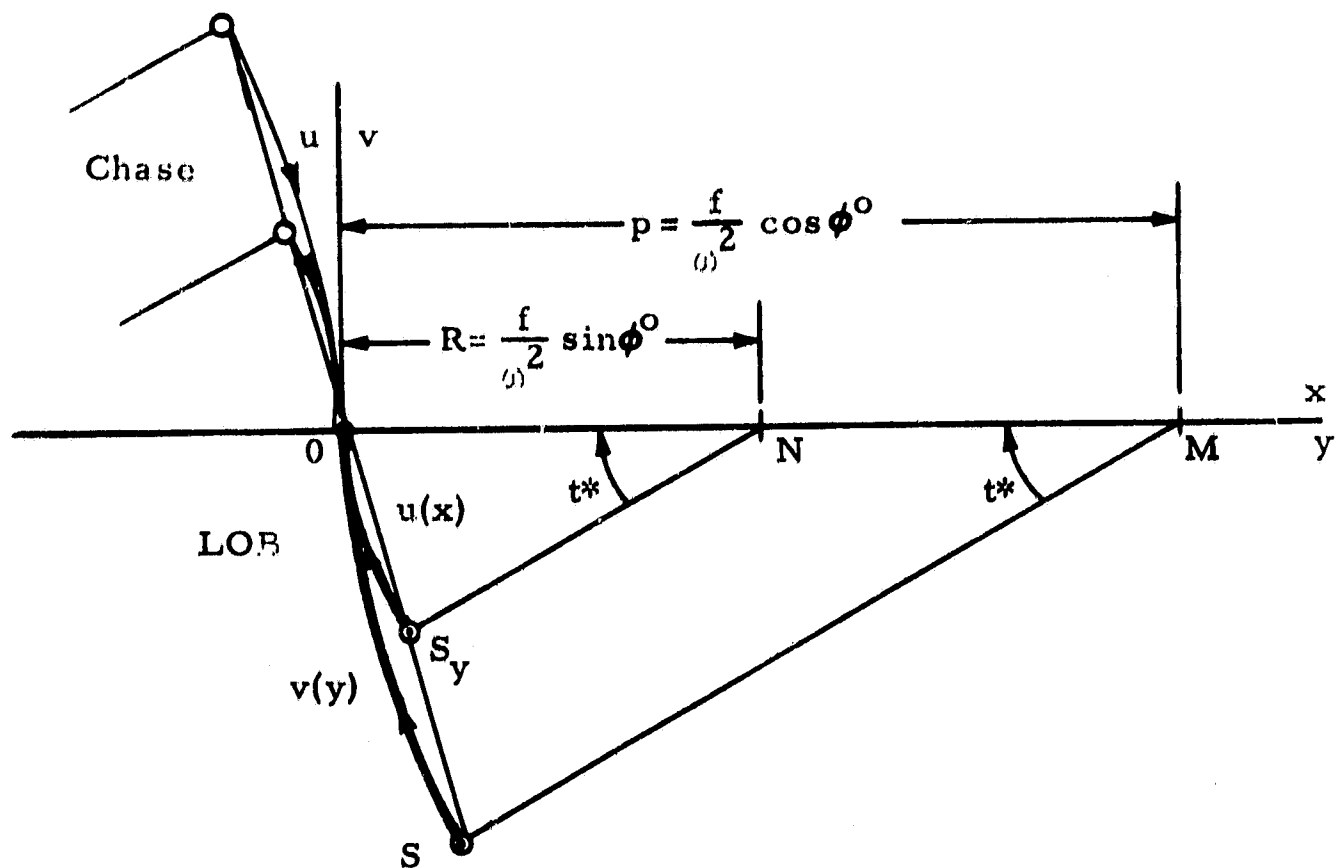


Figure 4 - Dual Phase Plane Representation of Terminal Powered Flight Phase Gained by Superposition of x, y and y, v Phase Planes. For short second burn times t^* the hyperbolic x, u path is approximated by circle. Phase points are aligned with origin throughout terminal powered flight:

$$xv - yu = 0 \quad \text{or} \quad \vec{r} \times \vec{s} = 0$$

If not all the optimality conditions $g = h = k = 0$, are simultaneously satisfied throughout the terminal powered flight phase, deviations from the optimal path result that must be determined and corrected if necessary.

4.2 SENSITIVITY OF THE OPTIMAL SOLUTION TO SMALL PERTURBATIONS

The sensitivity of the optimal trajectory to small perturbations is studied by first determining the divergence rates of the optimal conditions g , h and k if no corrective action is assumed. The derivatives with respect to $t^* = \omega t$ are:

$$\vec{r}^{\prime *'} = \begin{pmatrix} x^{\prime *} \\ y^{\prime *} \end{pmatrix} = \begin{pmatrix} -u^* + \frac{u}{x} f_x^* \\ -v^* + \frac{v}{y} f_y^* \end{pmatrix} \quad (4.27)$$

Assuming again a constant thrust vector during second burn yields

$$\begin{aligned} g' &= \vec{r}^{\prime *} \times \vec{f}^* \\ &= -\vec{s}^* \times \vec{f}^* - \frac{f_x^* f_y^*}{xy} \vec{r} \times \vec{s} \end{aligned} \quad (4.28)$$

$$h' = 2 \vec{s}^* \cdot (\vec{f}^* - \vec{r}^*) \quad (4.29)$$

Under the same restrictions to small burn times that were imposed on condition (4.24a), the derivative becomes

$$\tilde{k}' = \vec{r} \times \vec{f}^*. \quad (4.30)$$

Hence an optimal terminal flight path characterized by

$$g = h = k \equiv 0$$

during powered flight is stable in the presence of small perturbations if the time derivatives g' , h' , k' of Equations (4.28), (4.29) and (4.30) satisfy the inequalities:

$$\left. \begin{aligned} \text{sgn } g' &\neq \text{sgn } g \\ \text{sgn } h' &\neq \text{sgn } h \\ \text{sgn } \tilde{k}' &\neq \text{sgn } \tilde{k} \end{aligned} \right\} \quad (4.31)$$

A typical optimal vector configuration for the approach phase is shown in Figure 5, where it is assumed that the remaining burn time is sufficiently short to make the approximate relation (4.24a) valid.

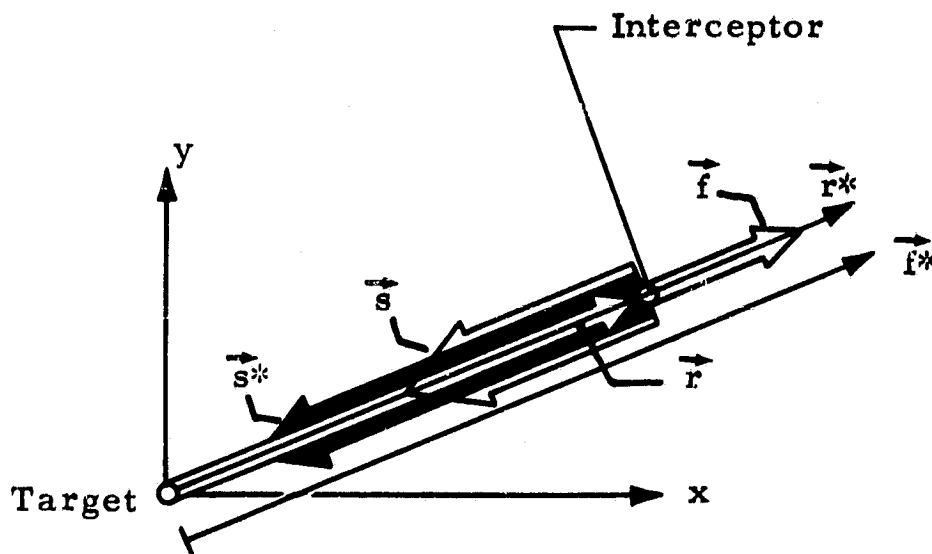


Figure 5 - Optimal Alignment of Range Vectors \vec{r} , \vec{r}^* Thrust Vectors \vec{f} , \vec{f}^* and Relative Velocity Vector \vec{s} During Terminal Powered Flight Phase

Note: For large \vec{r} or long second burn times \vec{r}^* and \vec{f} are not aligned with \vec{r} .

This configuration is characterized by

$$\vec{r}^* \parallel \vec{f}^* \quad \text{for} \quad g = 0$$

$$r^* = f^* \quad \text{for} \quad h = 0$$

$$\vec{r} \perp \vec{s} \quad \text{for} \quad \tilde{k} = 0$$

At the same time all the derivatives vanish:

$$g' = h' = \tilde{k}' = 0 .$$

4.3 CONTROL LAWS FOR SENSITIVITY REDUCTION

The above relations (4.23) through (4.31) have been used to derive compensation schemes for correcting the flight path if one or several of the conditions for optimal terminal flight are violated (Reference 6). A simple feedback law for thrust vector steering

$$\phi = \arctan \frac{y^*}{x^*} - K_\phi \arcsin \frac{\vec{r} \cdot \vec{x} \cdot \vec{s}}{rs} \quad (4.32)$$

has been found to effectively correct small perturbations

$$g \neq 0 \quad \text{and} \quad k \neq 0$$

if the gain K_ϕ is properly chosen. A region for optimal gains K_ϕ , which ensures compensation of limited disturbances within the remaining burn time, was established (Reference 7). Under the simplifying assumption of small deviations from the optimal trajectory and assuming ideal inertialess thrust vector steering, a lower bound

$$K_{\phi \min} = 4$$

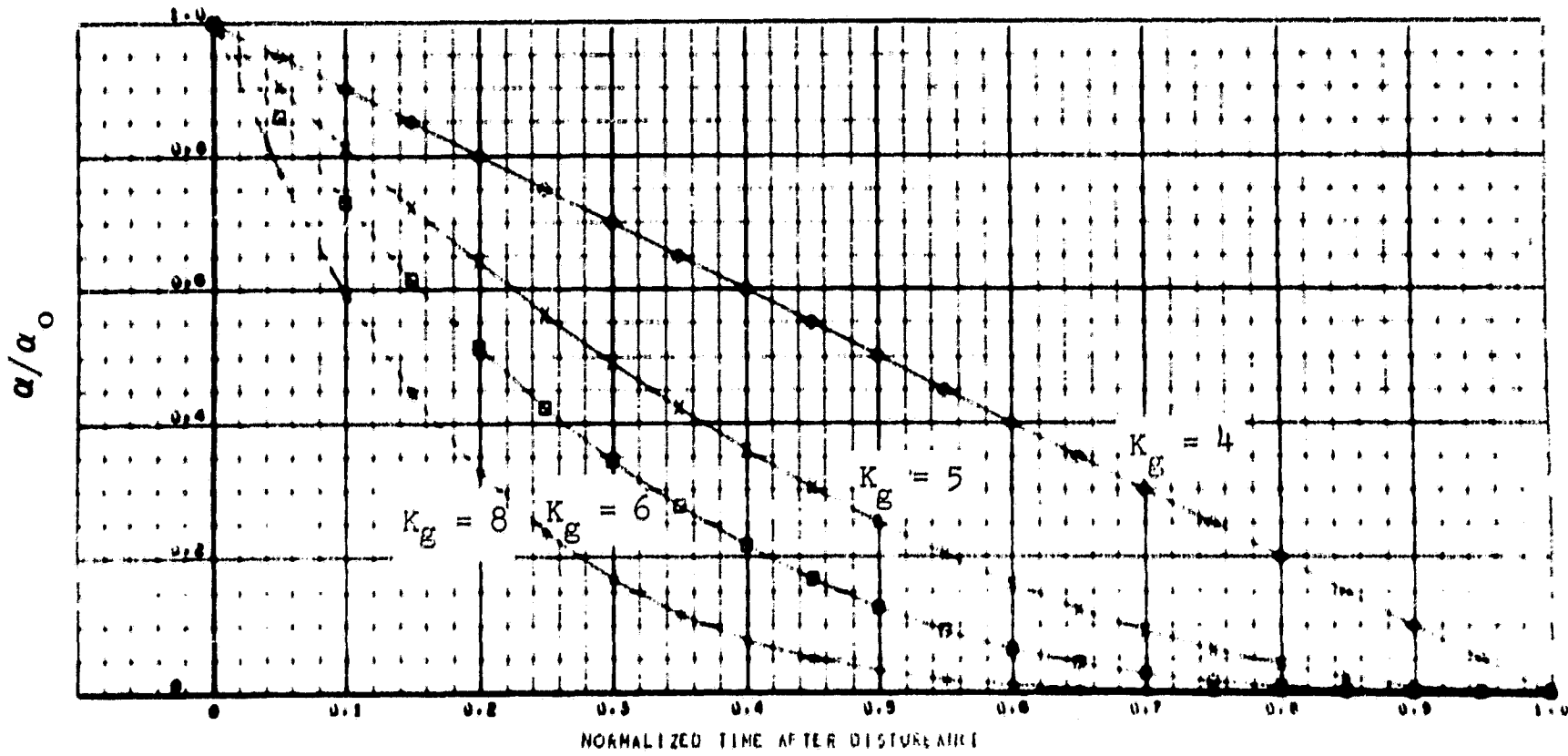


Figure 6 - Compensation of Initial Misalignment α_0 by Thrust Deflection $\Delta\phi = K_g \alpha$, where $\alpha \triangleq \arcsin \frac{\vec{r} \times \vec{s}}{rs}$

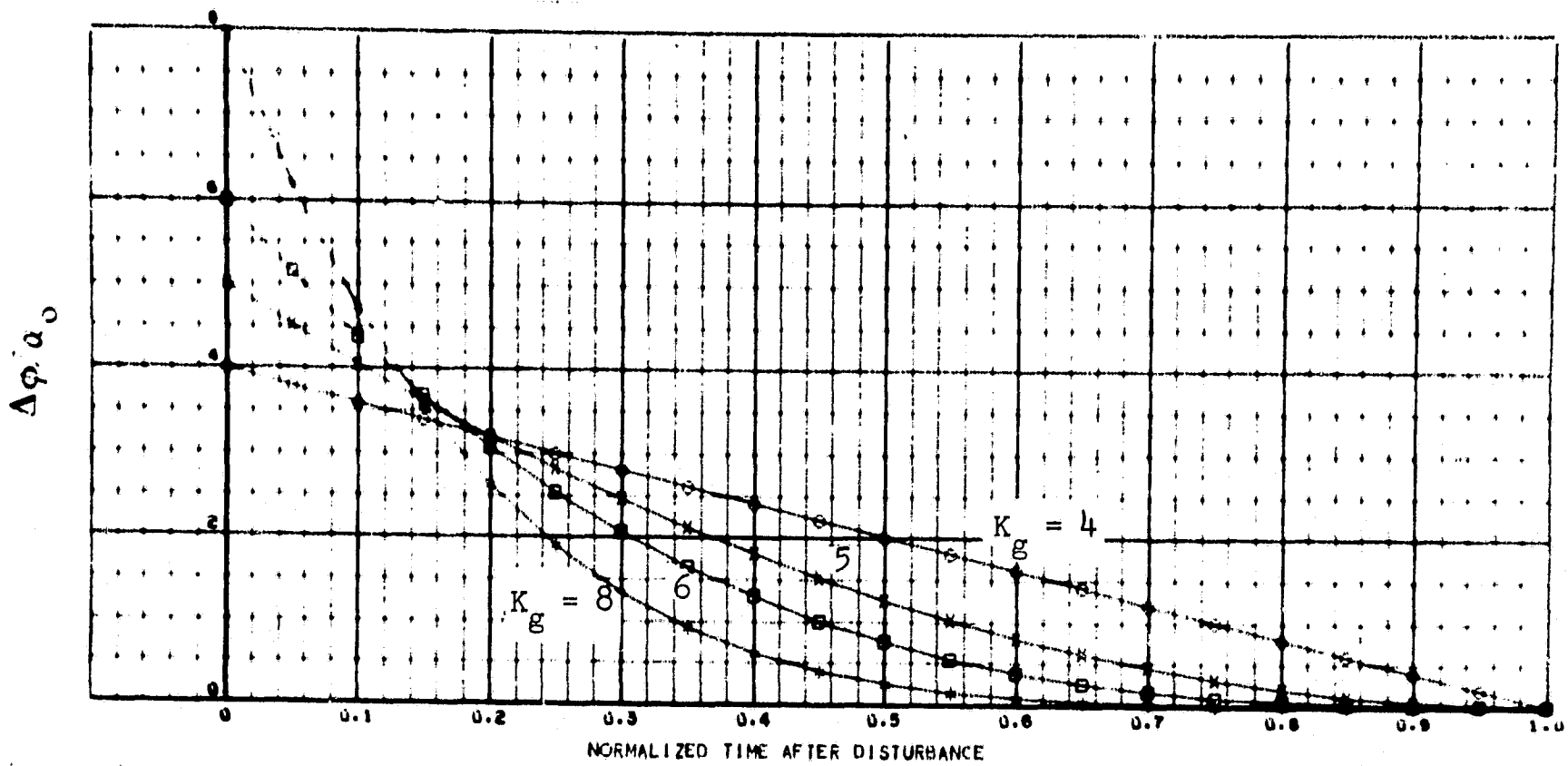


Figure 7 - Required Thrust Deflections to Compensate Misalignment α Between \vec{r} and \vec{s}

was found and closed-form solutions for the resulting corrective maneuvers were derived in Reference 7. In Figures 6 and 7, transients are plotted for various gains in nondimensional form. The marginal case $K_g = 4$, also included, does not correct the misalignment α until rendezvous at $\tau = 1$ (Figure 6) and results in a constant rotation of the vectors \vec{r} , \vec{s} and \vec{f} throughout the corrective maneuver, whereas the optimal case calls for space-fixed orientation of these vectors.

The final gain selection out of the region $K_g > 4$ requires a tradeoff between rapid convergence to optimal alignment (as obtained from high gains) and the admissible thrust vector deflections $\Delta\phi$ which result in high peaks for large gains as is shown in Figure 7. It should be considered, however, that these peaks will be less pronounced in an actual system due to the finite time constants of the thrust deflection mechanism, which were neglected in this idealized approach.

The complete set of terminal guidance equations consisting of the switching function (4.23), the control law (4.32) and the associated transformations (4.20) are compiled in the block diagram, Figure 8. This scheme has been extensively tested in simulated approach phases of a rendezvous mission. Results of these simulations are given in Section 5.

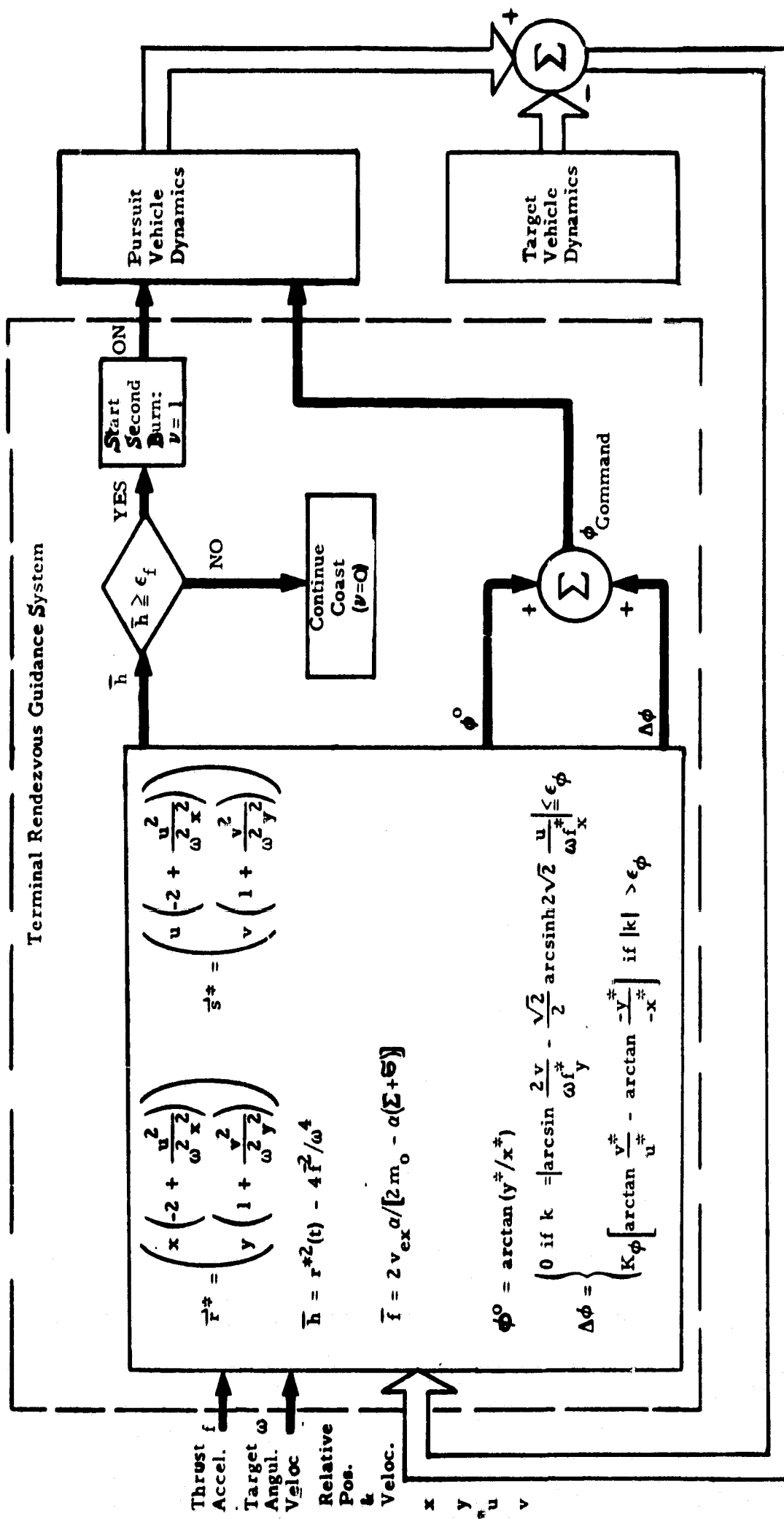


Figure 8 - Block Diagram of Closed-Loop Terminal Rendezvous Guidance System for Second Burn

Section 5

SIMULATION RESULTS

The above guidance schemes have been checked in a computer simulation of entire rendezvous missions. Such a mission starts with the flight scheduling operation which provides predictions of the location of the rendezvous. This makes it possible to specify the Cartesian coordinate system used during the second burn. Then the first burn guidance scheme steers the interceptor onto a coasting ellipse, from which the second burn control method is able to achieve rendezvous.

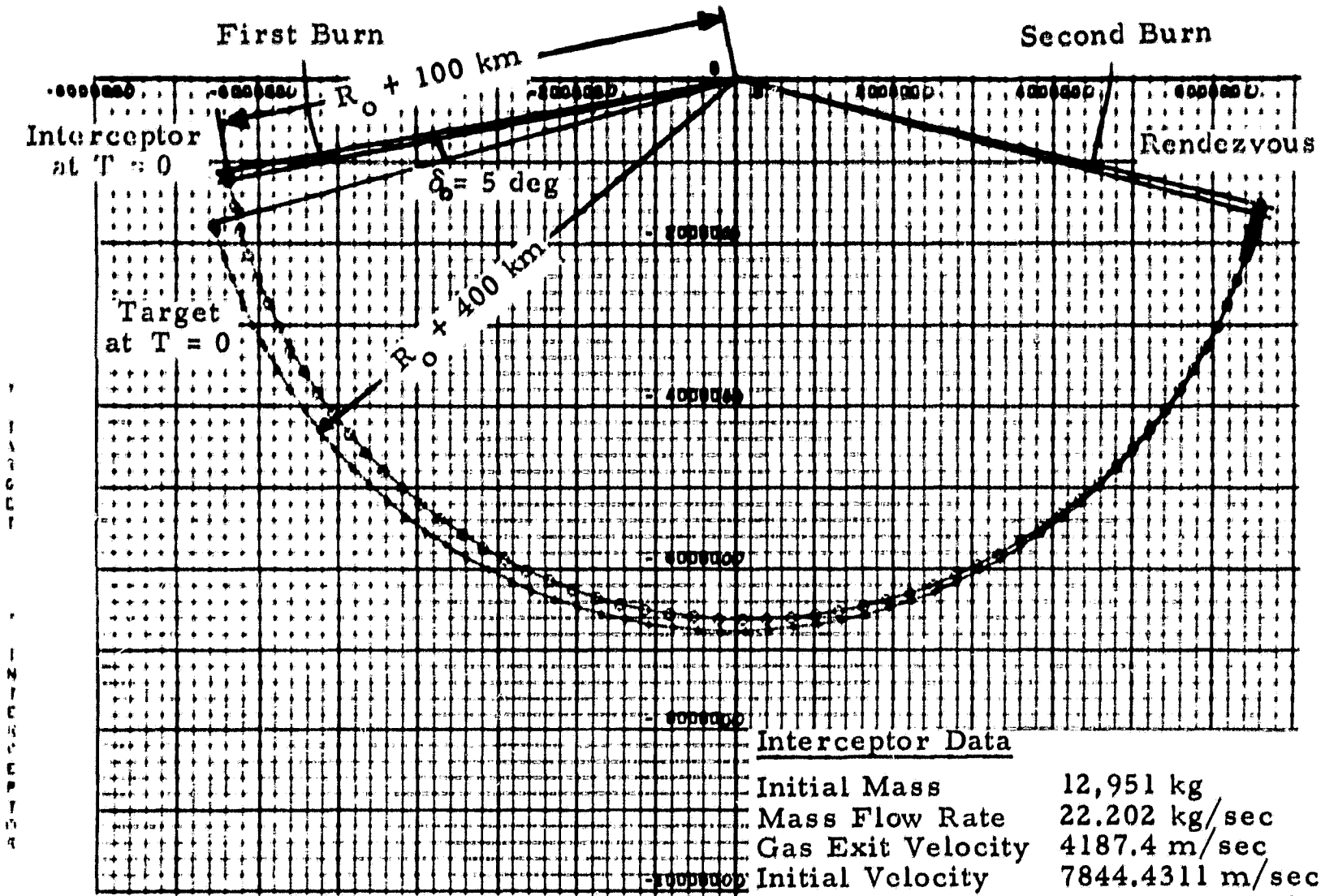
The simulation program imitates all events of the flight. During the burn phases the program evaluates the input parameters to be processed by the control subprogram and determines the current values of the control parameters by carrying out the proposed on-board computations. The cycle is closed by the numerical integration of a small portion of the vehicles' trajectories. The time increment is equal to the on-board computing time for one set of control variables (here .15 sec).

In the following graphs we display the results from the simulation of a "Hohman-transfer-like" rendezvous with comparatively short burn durations (1 percent of the flight duration). The initial altitude difference of the two vehicles was assumed to be 300 km, and the interceptor was initially on a circular parking orbit, and its engine was characterized by $\lambda = 22.20$ kg/sec, $v_x = 4187$ m/sec, $m_0 = 12951$ kg. Figure 9 shows the gross situation at this rendezvous.

The two-dimensional minimum problem involved in the first burn guidance was solved with sufficient accuracy within four iteration steps starting from rather poor initial guesses.

The performance of the terminal guidance scheme under optimal first burn and coast conditions is shown in Figures 10 and 11 where all relative positions and velocities are simultaneously reduced to near-zero values.

Simulation of the same mission using the first burn control variables as computed by the near-optimal first burn guidance scheme results in substantial deviations from the optimal trajectory at the end of the coast period. Under such non-optimal conditions the terminal guidance scheme yields near zero terminal errors for both relative velocities and one position coordinate only. The second position coordinate - $x(t_3) = 394$ meters in the example - must be zeroed during the docking phase.



Comparison of Trajectory Data

	Present Guidance Scheme	Optimal COV Solution
First Burn Time σ	13.3 sec	13.29 sec
Coast Time	2318.4 sec	2522.7 sec
Second Burn Time τ	12.1 sec	11.97 sec
Thrust Angles χ_0	62.8°	64.9°
χ_1	62.8°	65.2°
χ_2	90.0°	73.9°
χ_3	90.0°	74.4°

Figure 9 - Simulated Rendezvous Mission of Short Burns Compared with Optimal Solution Gained from a COV Computer Program

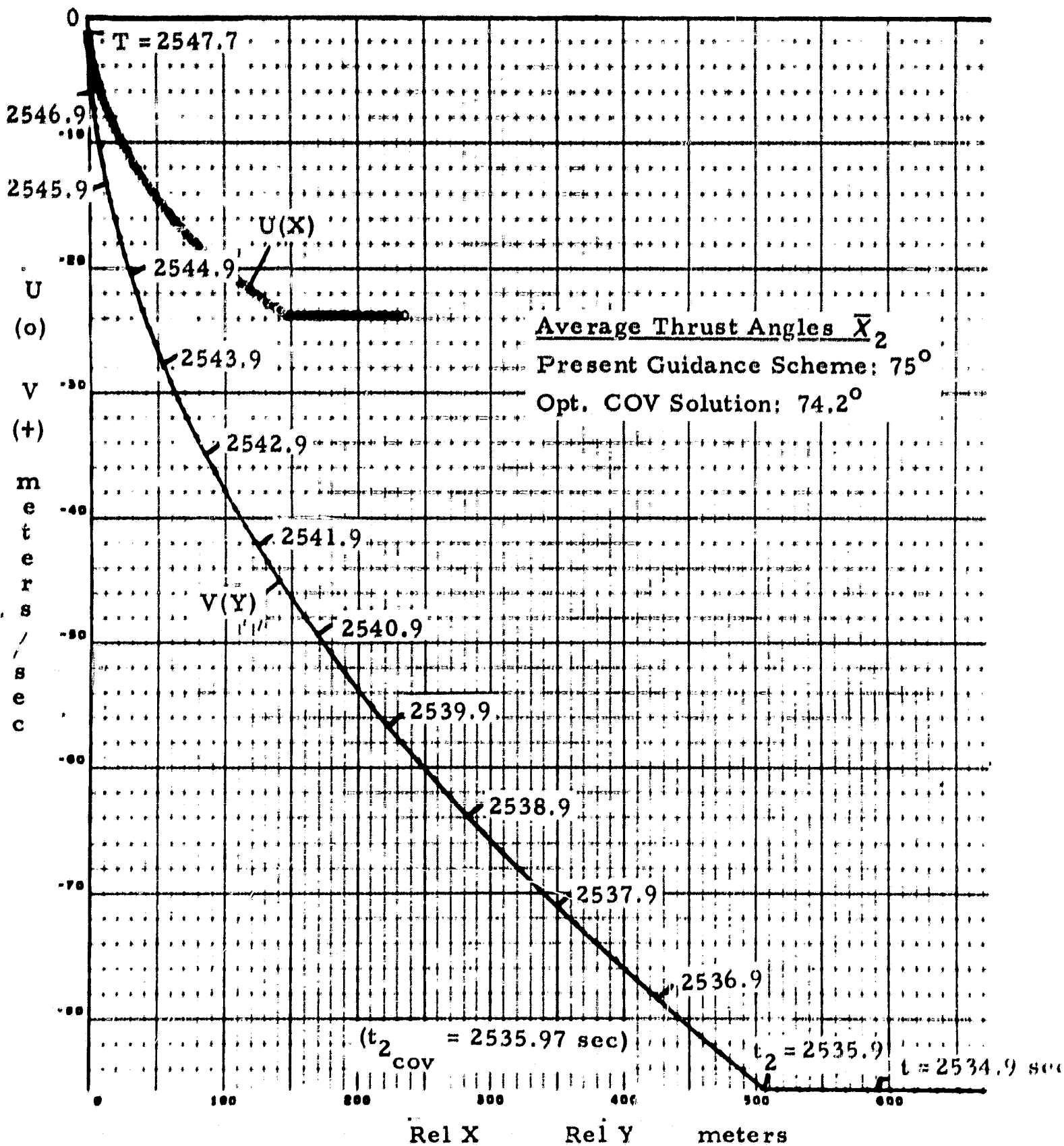


Figure 10 - Second Burn Flight in Dual Phase Plane Representation Starting from Optimal (COV) Coast Trajectory. All Relative Velocities and Positions are Simultaneously Reduced to Near-Zero Values.

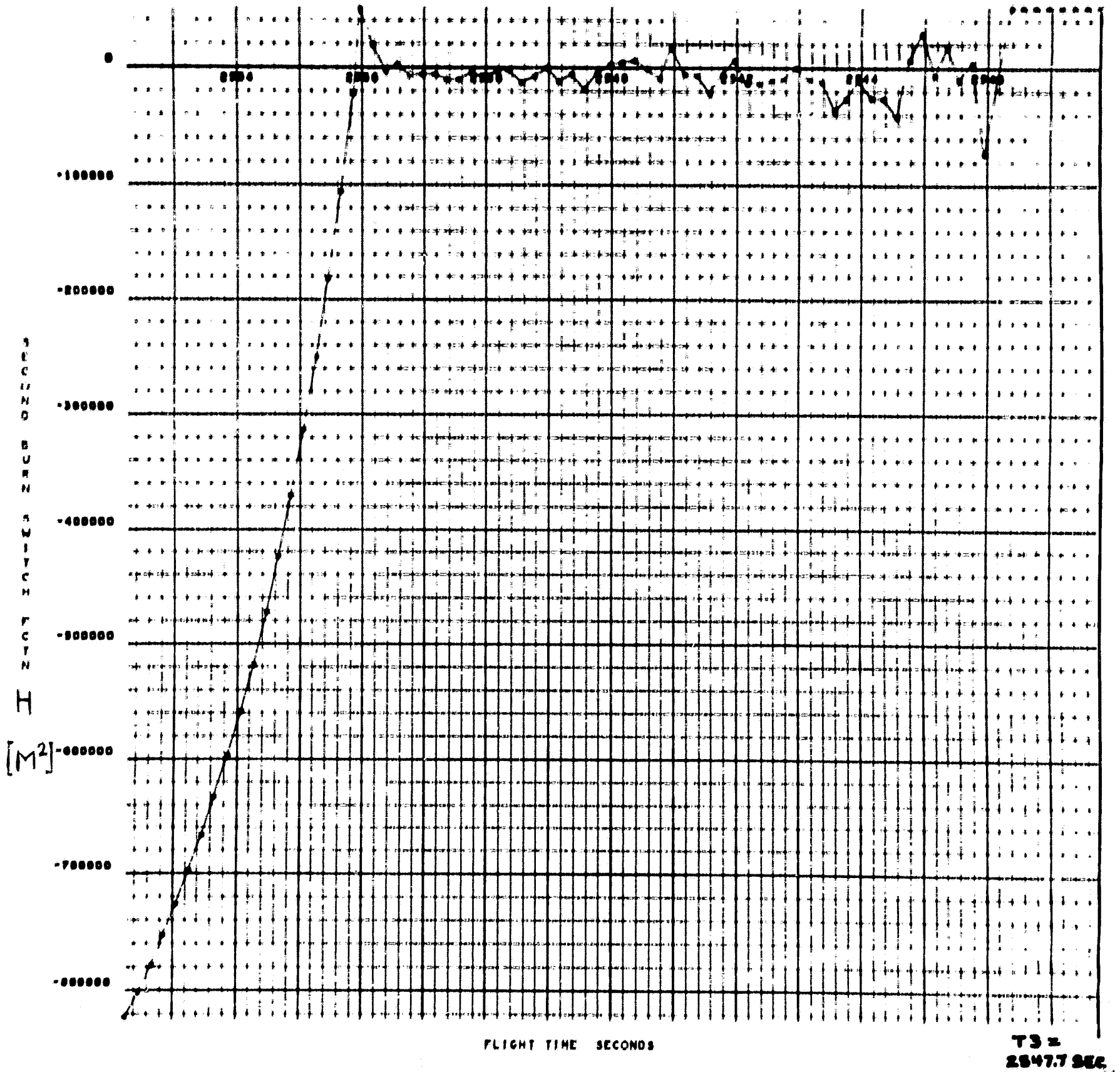


Figure 11. - Switching function h versus time in the final phase of the rendezvous assuming optimal first burn and coast phases.

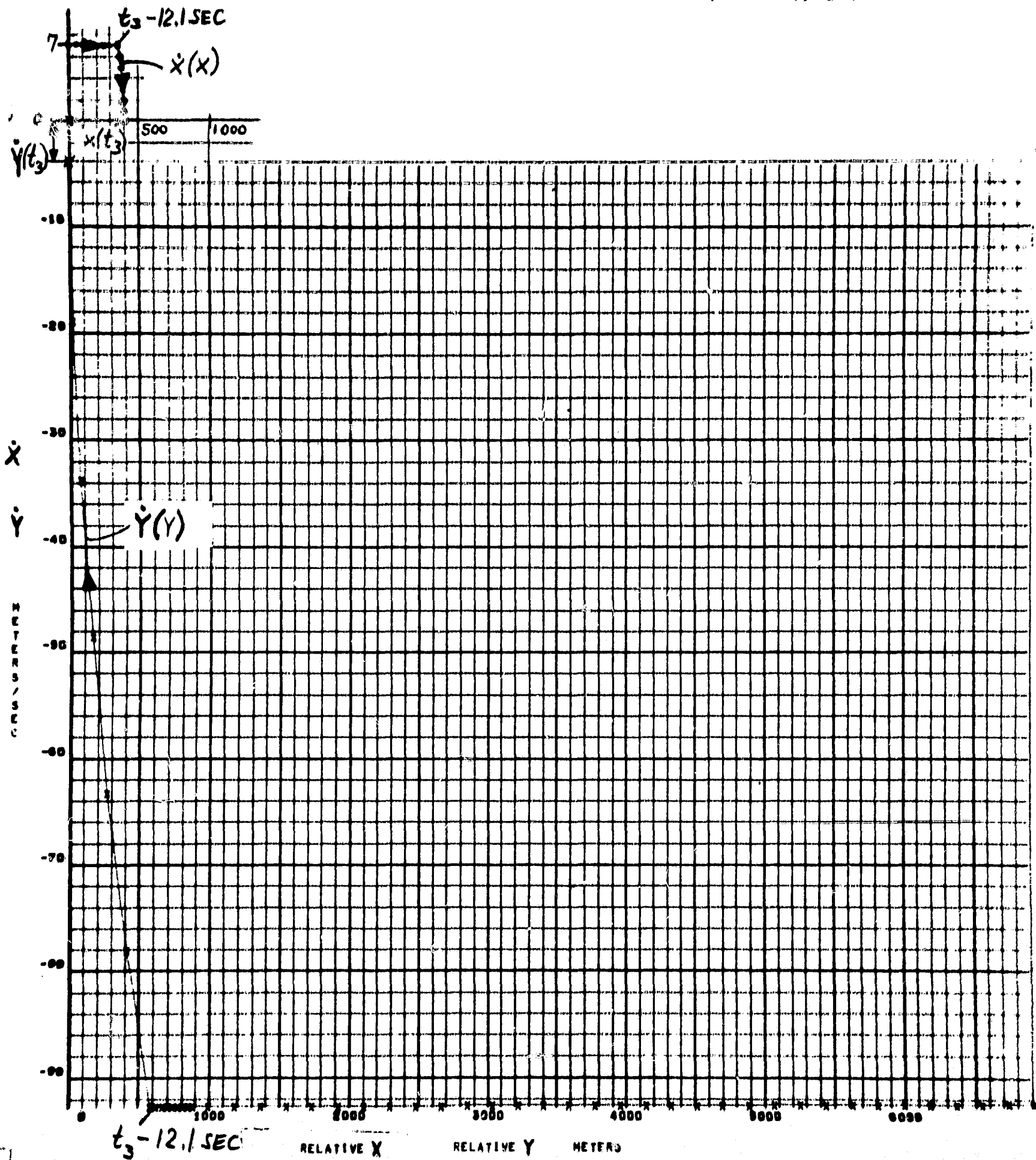


Figure 12 - Terminal Phase of Simulated Total Mission with Non-Optimal First Burn and Coast Trajectory. Deviations from optimal first burn and coast phase result in finite terminal error of one position coordinate.

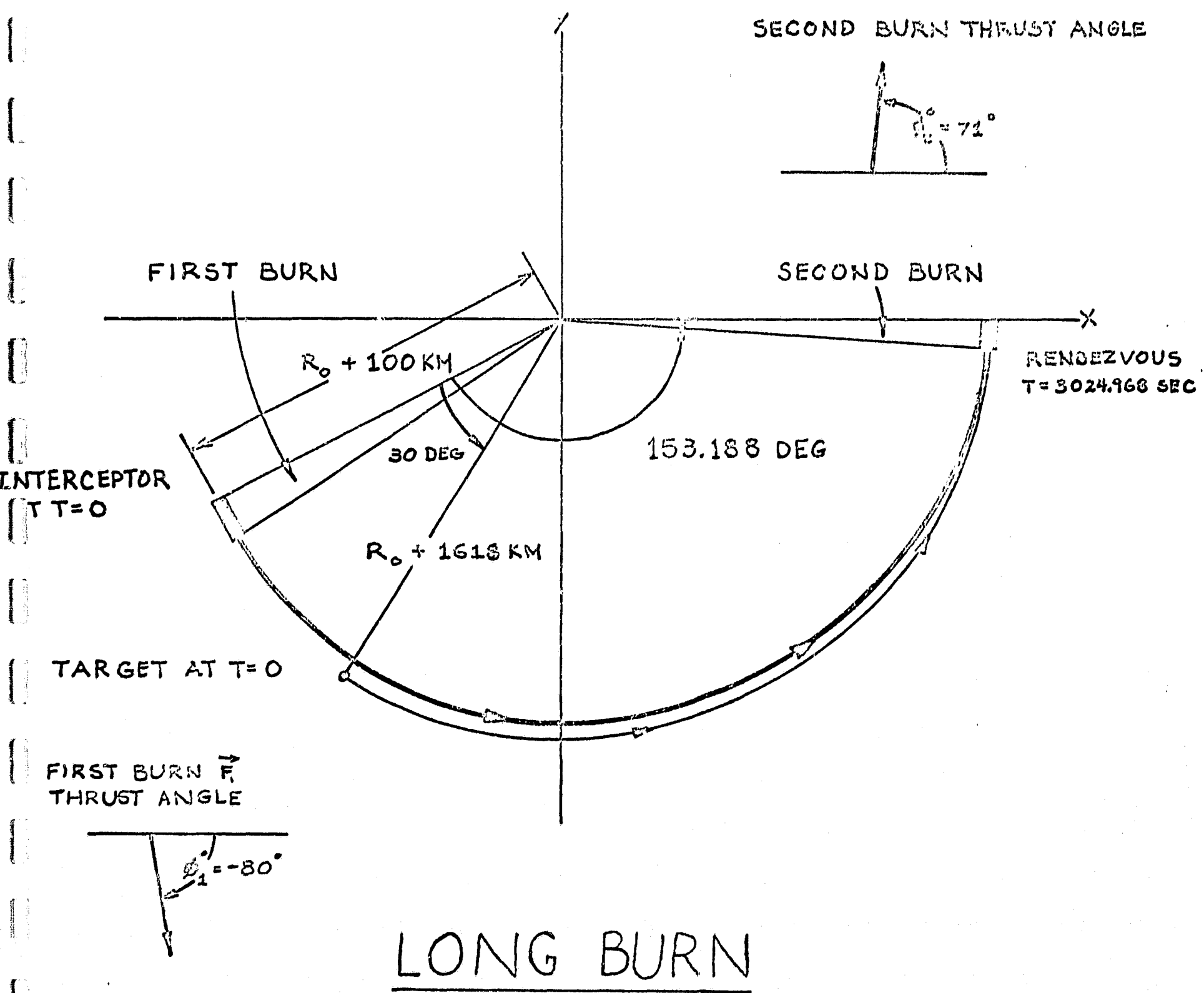


Figure 13

Figure 13 shows a rendezvous using the same interceptor. The initial altitude difference was 1518 km, which caused the burn durations to increase up to about 3 percent of the flight duration.

REFERENCES

1. Kliger, I., "Dual Phase Plane Approach to the Two-Finite-Burns Minimum Fuel Rendezvous Problem," TM-54/30-116, LMSC/HREC A783413, November 1966.
2. Stiefel, E., "Many Body Problems and Interplanetary Flight," Dynamics of Rockets and Satellites, Editor: G. V. Groves, New Holland, 1965.
3. Waldvogel, J., "Simplified Guidance Laws for the Planar Two-Finite Burns Minimum Fuel Rendezvous Problem," TM-54/30-150, LMSC/HREC A784607, Lockheed Missiles & Space Company, Huntsville, Alabama, July 1967.
4. Kliger, I. E., "Rendezvous Guidance Study" Final Report, Contract NAS8-18036, LMSC/HREC A783890, January 1967.
5. Clohessy, W. H. and R. S. Wiltshire, "Terminal Guidance System for Satellite Rendezvous," J. Aerospace Sci., Sept. 1960.
6. Trautwein, W., "Closed-Loop Terminal Guidance for the Two-Finite-Burns Minimum Fuel Rendezvous Problem," TM-54/30-151, LMSC/HREC A784608, July 1967.
7. Trautwein, W., "Dynamic Analysis of Closed Loop Terminal Rendezvous Guidance Scheme," Tech. Note, LMSC/HREC, October 1967.
8. Waldvogel, J., "The Minimization of the Fuel Consumption in the First Burn of a Planar Two-Burns Rendezvous," Tech. Note 54/30-12, LMSC/HREC A791148, Feb. 1968.
9. Trautwein, W., "Extension of the Dual-Phase Plane Terminal Guidance Method to Long Burn Times," Tech. Note 54/30-13, LMSC/HREC A791235, Feb. 1968.